Chemical Physics 178 (1993) 25–38
North-Holland

An investigation of the outermost orbital momentum distributions of formaldehyde, acetaldehyde and acetone, by electron momentum spectroscopy and quantum chemical calculations at the SCF and MRSD-CI levels

B.P. Hollebone, P. Duffy, C.E. Brion
Department of Chemistry, University of British Columbia, 2036 Main Mall, Vancouver, British Columbia, Canada V6T 1Z1

Y. Wang and E.R. Davidson
Department of Chemistry, Indiana University, Bloomington, IN 47405, USA

Received 21 July 1993

The outermost valence electron momentum profiles have been obtained at high-momentum resolution for acetone ($5b_2$) and acetaldehyde (10a′). These are compared with calculated profiles of wide ranging quality from minimal basis STO-3G to near Hartree–Fock limit SCF treatments, together with the outermost momentum profile of formaldehyde ($2b_2$) measured previously by Bawagan et al. (Chem. Phys. 128 (1988) 439). The effects of the addition of diffuse functions to the basis sets are examined for a number of properties. Many-body corrections to the independent particle SCF model are evaluated by multi-reference singles and doubles configuration interaction calculations of all three molecules. These are found to give large improvements for calculated total energy but only modest gains in agreement with the observed momentum profiles. The implications for the nature of chemical bonding in these orbitals is discussed in the context of the theoretical and experimental results.

1. Introduction

A detailed description of molecular electronic structure is necessary to understand chemical properties and reactivity. In particular, it is important to obtain good descriptions of the electron density (the square of the quantum mechanical wavefunction) over all regions of space including the "long-range" or "large-r", low-momentum regions that play an important role in determining the chemical activity. It is therefore important to obtain a good description of the electron density distributions in both position and momentum space to fully appreciate a compound's behaviour. The frontier molecular orbital theory of Fukui [1], Woodward and Hoffmann [2] has emphasized the importance of the role of the electron density of the highest-occupied molecular orbital (or HOMO) in determining reactivity.

In addition to theoretical methods, the electron densities of individual orbitals can be experimentally investigated by electron momentum spectroscopy (EMS) [3,4]. This sensitive technique provides individual "orbital images" in momentum space, to a very good approximation. Thus, EMS can be used as an exacting experimental test of calculated molecular wavefunctions and provide a unique probe of the chemically important, spatially extended regions of the electronic densities. Several recent EMS measurements together with sophisticated ab initio molecular calculations [4–10] have shown that very accurate quantitative descriptions of the valence electron densities are now both experimentally and theoretically possible.

Recently, in this laboratory and elsewhere, the effects of alkyl- and fluoro-substitution on the HOMOs of amines [11–15] and the increasingly methylated H_2O [8], CH_3OH [16] and $(CH_3)_2O$ [17,18] series have been studied using both EMS and ab initio methods with a view to investigating the electron withdrawing behaviour of the alkyl groups on the

hetero atom "lone pair" (HOMO) electrons. In these studies the EMS and theoretical results, consistent with a growing body of other experimental evidence, such as NMR chemical shifts and dipole moments, clearly indicated that the methyl groups are intrinsically electron withdrawing (when compared with hydrogen) in contrast to traditional, intuitive arguments (see, for example, ref. [19]).

In the present work, these studies are extended to investigate the effects of methyl substitution on the carbonyl (C=O) functional group. Molecules of this type, aldehydes and ketones, are of particular interest to quantum chemistry because the electronic environment about the carbonyl group is uniquely electropositive when compared with other carbon environments. The study of the electron densities of series of increasingly methylated formaldehyde (H_2CO), acetaldehyde (CH_3CHO) and acetone ($(CH_3)_2CO$) can provide an improved understanding of both the "methyl inductive effect" and the fundamental difference between aldehydes (H_2CO, CH_3CHO) and ketones ($(CH_3)_2CO$). The experimental momentum profiles (XMP) of the outermost valence electrons of acetone ($(CH_3)_2CO$) and acetaldehyde (CH_3CHO) have been obtained by electron momentum spectroscopy. These experimental results, together with the outermost XMP of formaldehyde (H_2CO) obtained by Bawagan et al. [20], are compared with calculations of the theoretical momentum profiles (TMP) using a wide range of calculations including new near Hartree–Fock quality SCF and multiple reference single and double excitation configuration interaction (MRSD-CI) treatments. Other calculated molecular properties are also compared with experimental values in order to test all parts of the electronic wavefunctions [9]. In addition the effects of diffuseness are examined for intermediate quality SCF basis sets for all three molecules. These measurements and calculations provide the basis for discussion of the differences observed in the electronic structure of the HOMO oxygen "lone-pairs" in both position and momentum space with increasing methyl substitution of the C=O group. Particular attention is given to the effects of orbital symmetry and the nature of chemical bonding in the outermost orbital in the context of the EMS measurements and the new ab initio calculations.

2. Method

A detailed description of the EMS spectrometer has been given elsewhere [21]. In brief, gaseous target molecules are ionized by impact with a 50 μA electron beam of defined energy ($E_0 = 1200$ eV + binding energy). Both of the outgoing electrons (scattered and ionized) are angle and energy selected and detected in coincidence. The experimental geometry used is referred to as symmetric non-coplanar, that is, the two outgoing electrons are selected to have equal energies ($E_1 = E_2 = 600$ eV) and equal polar angles ($\theta_1 = \theta_2 = 45°$) relative to the forward scattered electron beam. The relative azimuthal (out of plane) angle ϕ_0 between the two outgoing electrons is variable. Under the approximations of high impact energy and negligible kinetic energy transfer to the resultant ion, the initial momentum (in the molecule) of the knocked-out, ionized electron can be shown to be almost linearly related to the azimuthal angle [3,6]

$$p = (2p_1 \cos\theta_1 - p_0)^2 + [2p_1 \sin\theta_1 \sin\theta_1 \sin(\tfrac{1}{2}\Psi_0)]^{1/2}, \quad (1)$$

where $p_1 = p_2 = \sqrt{2E_1}$ is the magnitude of the momentum of the two outgoing electrons and $p_0 = \sqrt{2E_0}$ is the momentum of the incident electron.

The EMS binary (e,2e) triple differential cross section in the plane wave impulse approximation (PWIA) for randomly oriented gas-phase molecules is [6]

$$\sigma_{\mathrm{EMS}} \propto \int \mathrm{d}\Omega \, |\langle \boldsymbol{p}\, \Psi^{(N-1)} | \Psi^{(N)} \rangle|^2, \quad (2)$$

where $\boldsymbol{p}$ is the momentum of the target electron state prior to knockout and $\Psi^{(N-1)}$ and $\Psi^{(N)}$ are the final ion and molecular target wavefunctions respectively. From this formulation the ion–neutral overlap distribution (OVD) is calculated, which is necessary when using manybody calculations for the initial and final wavefunctions, such as configuration interaction treatments.

In the target Hartree–Fock approximation (THFA) the initial state wavefunction is approximated by the SCF wavefunction. If the ion state is dominated by a single hole in only one orbital, eq. (2) can be simplified to

$$\sigma_{\mathrm{EMS}} \propto S_i^{(f)} \int \mathrm{d}\Omega \, |\psi_i(\boldsymbol{p})|^2, \qquad (3)$$

where $\psi_i(\boldsymbol{p})$ is the momentum representation of the more familiar position space molecular orbital wavefunction, $\psi_i(\boldsymbol{r})$, which corresponds to the orbital from which the electron was ionized. The spherically averaged square of the $\boldsymbol{p}$-space molecular orbital (eq. (3)) is referred to as a momentum distribution. The quantity $S_i^{(f)}$ is called the spectroscopic factor and is the probability of the ionization event producing a $(\Psi_i)^{-1}$ one-hole configuration of the final ion state, $\Psi^{(N-1)}$. In the Koopman approximation of the ion state, $S_i^{(f)} = 1$.

In EMS the individual orbitals are selected by the choice of the binding (or ionization) energy. A differential cross section is obtained by measuring the true electron coincidence counts at a constant impact energy (1200 eV + binding energy) and varying ϕ_0, the relative azimuthal angle between the outgoing electrons, and therefore the initial momentum of the target electron (as described by eq. (1) above). The energy resolution of the spectrometer is 1.7 eV fwhm, which allows for full binding energy resolution of the outermost orbital of all three systems investigated in the present work. The angular resolution is $\Delta\theta \approx \pm 1.0°$ and $\Delta\phi_0 \approx \pm 0.6°$, which gives an approximate momentum resolution of 0.1 atomic units [22].

The acetone and acetaldehyde samples used were spectroscopic grade (>99.9% pure) from BDH chemicals. Gaseous impurities dissolved in the samples were removed by repeated freeze–thaw–pump cycles using liquid nitrogen. To avoid pressure variations in the samples, both molecules were kept at 0°C by immersion of the sample tube in an ice bath which maintained the target gas pressures at a constant 1.5×10^{-5} Torr.

3. Calculations

Spherically averaged theoretical momentum profiles (TMPs) have been calculated from several basis sets of varying quality using Koopmans theorem and the target Hartree–Fock approximation (eq. (3)). In addition, full ion–neutral overlap distributions have been calculated from the plane wave impulse approximation of the EMS cross section (eq. (2)) using multi-reference singles and doubles excitations configuration interaction (MRSD-CI) calculations of both the ground state and molecular ions to investigate the effects of correlation and relaxation on the wavefunctions. The MRSD-CI calculations were based on the single determinant near-Hartree–Fock limit basis sets for the respective molecule and used neutral molecule orbitals for both the neutral and ion. The instrumental angular (momentum) resolution was included in the calculations using the Gaussian-weighted planar grid method of Duffy et al. [22].

The smaller, more limited calculations were done at the experimental geometries obtained from averaged rotational (microwave) spectroscopic data (formaldehyde) [23] and zero-point average structures measured by both electron diffraction and microwave rotational spectroscopy for acetone [24] and acetaldehyde [25]. Although these studies determined the C–H bond lengths for the methyl groups of both acetone and acetaldehyde, the orientation of the freely rotating methyl groups on both CH_3CHO and $(CH_3)_2CO$ were not determined. The methyl group for acetaldehyde was chosen to be in an eclipsed conformation with respect to the carbonyl group. For acetone, the methyl geometries were chosen to be in a "half-staggered" conformation (one methyl eclipsed, the other anti to the C=O bond). Previous studies on dimethyl ether [18] have shown that methyl group orientation has only a small effect on the resulting TMPs at this level of calculation.

For the near-Hartree–Fock limit level basis sets, a geometry optimization was done on the basis sets to investigate the energy differences of the rotational conformers of acetone and acetaldehyde using 6-31G** basis sets at the Hartree–Fock second-order Møller–Plesset perturbation theory (MP2) level. Acetaldehyde was found to have two minimum energy C_s structures. The "staggered" form has one C–H bond anti to the C=O. The "eclipsed" conformer has one C–H bond eclipsing the carbonyl group (very similar to the geometry used for the smaller calculations, described above). The eclipsed form was found to be 1.6 mhartree lower in energy than the staggered form at the 6-31G**/MP2 level. Acetone had three energy minima structures, two with C_{2v} symmetry, one with C_s. All three forms were found to have one C=H bond in each methyl group in the (C_2C=O) molecular plane. The "eclipsed" form has both in-plane

C–H bonds eclipsed with C=O bond; the "staggered" form has the in plane C–H bonds anti to the ketone C=O bond; the "half-staggered" conformer has one C–H bond eclipsed and one anti. The "half-staggered" conformer was very similar to that used for the smaller calculations. The eclipsed form was found to be the lowest-energy structure with the half-staggered being 1.2 mhartree higher in energy and the staggered form 3.6 mhartree less stable according to the 6-31G**/MP2 calculations. The eclipsed geometries were used for the near-Hartree–Fock and subsequent MRSD-CI calculations for both acetone and acetaldehyde.

Details of the calculation methods are described below and selected properties are given in table 1.

(1) STO-3G: In this minimal basis set each function is a contraction of three Gaussians, roughly equivalent to a single Slater-type function. The oxygen and

Table 1
Calculated and experimental properties of small C=O group compounds

Molecule		Basis set	Total energy (hartree)	Dipole moment [a] (D)	p_{MAX} (au)	
H_2CO [b]	1	STO-3G	−112.354	1.53	0.94	
	2	4-31G	−113.691	3.01	0.89	
	3	4-31G+sp+s	−113.699	3.16	0.88	
	4	Snyder and Basch (DZ)	−113.821	3.11	0.88	
	5	90-GTO	−113.917	2.94	0.84	
	6	142-GTO [c]	−113.918	2.86	0.84	
		Hartree–Fock limit [d]	−113.92	2.86		
	5c	90-G(CI)	−114.277	2.55	0.84	
	6c	142-G(CI) [c]	−114.276	2.45	0.84	
		experimental	−114.515 [e]	2.33 [f]	0.75	
CH_3CHO [g]	1	STO-3G	−150.940	1.77	1.20	
	2	4-31G	−152.690	3.40	1.10	
	3	4-31G+sp+s	−152.689	3.60	1.06	
	4	Snyder and Basch (DZ)	−152.730	3.56	1.06	
	5	143-GTO	−152.982	3.34	1.04	
	5c	143-G(CI)	−153.451	3.06	1.04	
		experimental		2.75 [h]	1.04	
$(CH_3)_2CO$ [i]	1	STO-3G	−189.534	1.91	0.35	1.39
	2	4-31G	−191.676	3.53	0.32	1.23
	3	4-31G+sp+s	−191.686	3.75	0.34	1.23
	4	Snyder and Basch (DZ)	−191.764	3.67	0.35	1.23
	5	196-GTO	−192.043	3.51	0.32	1.24
	5c	196-G(CI)	−192.629	3.29	0.32	1.23
		experimental		2.90 [j]	0.32	1.10

[a] Positive dipole moment indicates that the oxygen nucleus is negative (i.e. C^+O^-).
[b] Geometry for calculations 1–4, 6 and 6c based on microwave spectroscopic data [23], a zero-point averge. Calculations 5 and 5c based on 6-31G**/MP2 optimized geometry. See section 3.
[c] Ref. [20].
[d] Estimated Hartree–Fock energy limit [26].
[e] Non-relativistic, infinite mass energy [27].
[f] Ref. [28].
[g] Geometry for calculations 1–4 based on a gas,phase ERD and MW zero-point averge [24]. Calculations 5 and 5c based on 6-31G**/MP2 optimized geometry. See section 3.
[h] Ref. [29].
[i] Geometry for calculations 1–4 based on a gas-phase ERD and MW zero-point averge [25]. Calculations 5 and 5c based on 6-31G**/MP2 optimized geometry. See section 3.
[j] Ref. [30].

carbon centres both provide [2s, 1p], the hydrogen [1s]. This basis was designed by Pople and coworkers [31].

(2) 4-31G: This is a split valence basis which has a minimal, single function description of the O and C 1s cores and essentially a double zeta description of the valence shell. It was developed by Ditchfield et al. [32].

(3) 4-31G+sp+s: This is an extension to the 4-31G basis above, developed by Casida and Chong [33,34] and has been extensively studied in this laboratory on work on hydrogen sulfide [35] and dimethyl ether [18]. The addition of the extra diffuse functions, s and p on each oxygen and carbon centre and an s function on the hydrogens, has been found, particularly in the dimethyl ether study [18], to greatly increase the reproduction of "large-r" properties such as the EMS momentum profiles with little extra effort. The exponents used were 0.0946 for the diffuse O s and p functions, 0.123 for C 5, 0.0663 for C p and 0.036 for the additional H s Gaussian function exponent.

(4) Snyder and Basch: This is the Gaussian basis set of Snyder and Basch [36]. The oxygen and carbon atomic bases consist of 4s and 2p contracted Gaussians, two for each occupied orbital. Similarly the hydrogen basis uses 2s contractions. This basis has been shown to give very similar results to a calculation using two Slater-type functions per filled atomic orbital [36] and is thus referred to as a double-zeta basis.

(5) Near Hartree–Fock SCF: These calculations (90-GTO for formaldehyde, 143-GTO for acetaldehyde and 196-GTO for acetone) were based on the highly converged, Gaussian function basis sets of Partridge [37]. These bases were energy optimized to within 4 μhartree of the (numerical) Hartree–Fock atomic limit. For C and O the original (18s, 13p) bases were contracted to [6s, 7p]. The hydrogen (10s) basis of Partridge [38] was contracted to [7s] Gaussian functions. The contraction scheme used lost less than 0.16 mhartree (0.1 kcal/mol) on trial SCF calculations of CO and CH_4 [15].

For better reproduction of the "large-r" properties, Dunning's "double d" polarization functions [39] were used for the O and C exponents (0.645, 2.314 and 0.318, 1.097, respectively). A single p polarization function was added to the hydrogens (exponent 1.30) [15]. A trial calculation on CO using this basis was within 3 kcal/mol of the numerical Hartree–Fock result.

(5c) MRSD-CI: The configuration spaces for the multi-reference singles and doubles configuration interaction calculations for both the molecular target and ion wavefunctions were chosen from the results of respective single reference singles and doubles configuration interaction perturbation calculations. For both the ion and neutral the molecular orbitals were from the neutral SCF wavefunction for which the virtual orbitals had been converted to K-orbitals [40–42] to improve the energy convergence. All CI calculations used frozen core electrons, to allow for the most detailed description of the valence electrons and most accurate reproduction of electronic properties possible at the current level of computation.

4. Results and discussion

4.1. Comparison of experimental and theoretical momentum profiles

High-momentum resolution measurements have been made of the outermost valence electron momentum profiles for each of acetone ($5b_2$) and acetaldehyde ($10a'$). These results are shown in figs. 1–3 together with the previously measured outermost XMP for formaldehyde ($2b_2$) [20]. On each figure the binding energy at which each particular XMP was measured is noted (9.7 eV for acetone, 10.2 eV for acetaldehyde and 10.9 for formaldehyde). These values correspond to the vertical ionization potentials of the lowest-lying peaks observed in the respective photoelectron spectra [43–45]. It should be noted that, for all three molecules studied, the outermost XMP is well separated in energy from the rest of the valence ionization manifold, which ensures that all the observed intensity of the momentum profiles is solely due to ionization to the lowest-lying ion state and contains no mixing with other ionization processes. Even for the smallest energy separation between the lowest and second lowest peaks in the photoelectron spectrum (in acetone $\approx$2.9 eV [43,44], the difference is still much greater than the instrumental energy resolution (hwhm $\approx$ 0.8 eV).

Each experimental momentum profile is compared in figs. 1–3 with the theoretical momentum

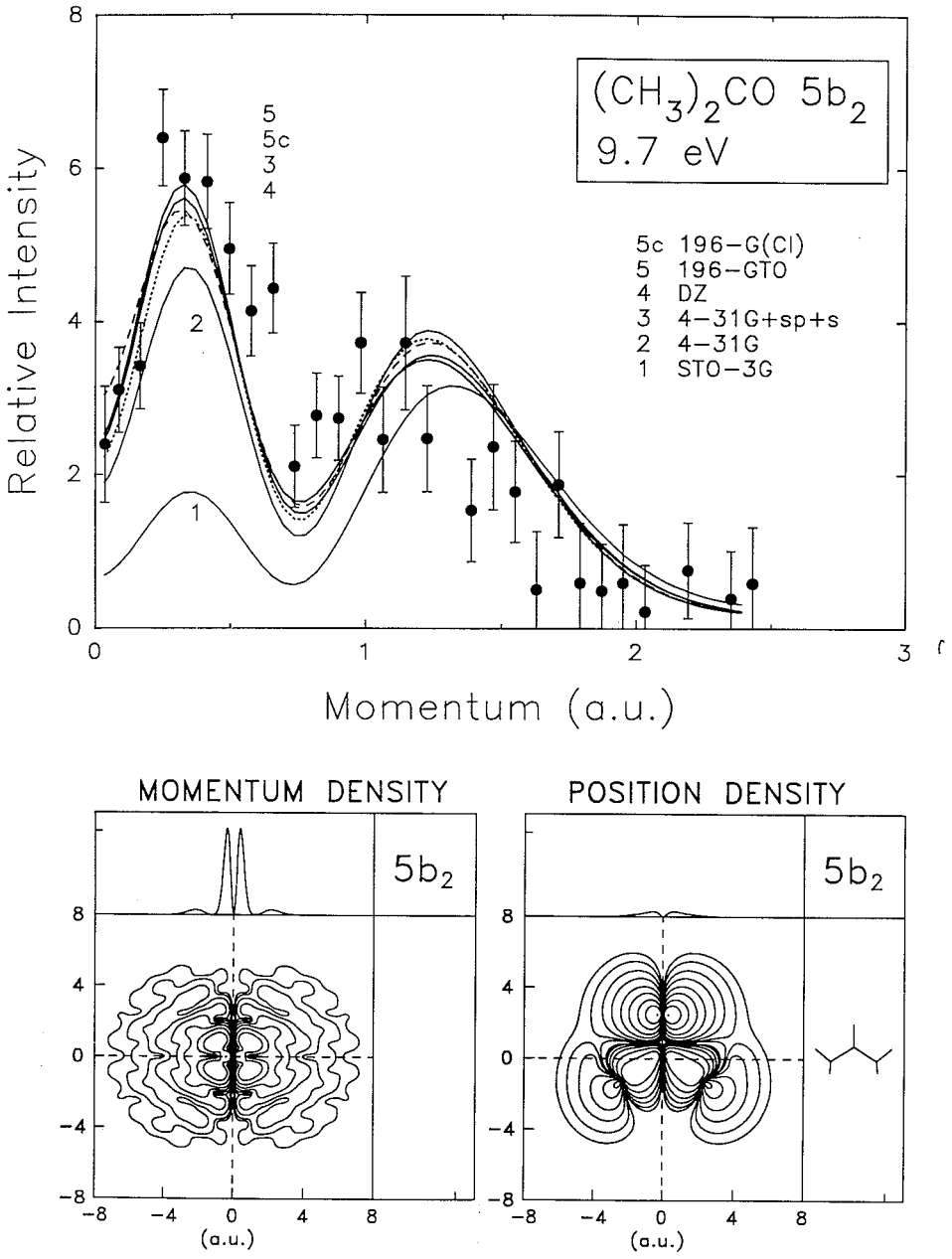

Fig. 1. Measured and calculated spherically averaged momentum profiles for the $5b_2$ electron of acetone (upper panel). The solid dots are the present experimental data. All calculations have been spherically averaged and folded with the experimental resolution using the GW-PG method [22] – see text (section 3 and table 1) for further details of the wavefunctions and normalization procedures. The lower panels show the momentum and position space density maps for an oriented $(CH_3)_2CO$ molecule calculated using the 196-GTO basis set (see section 3). The contours represent 0.01, 0.03, 0.1, 0.3,1.0, 3.0,10.0, 30.0, and 99.0% of the maximum density. The positions of the atoms on the position density plot (lower right panel) are located on the map. The side panels (right and top) show the density slices along the origin lines (dashed vertical and horizontal lines) for each density map.

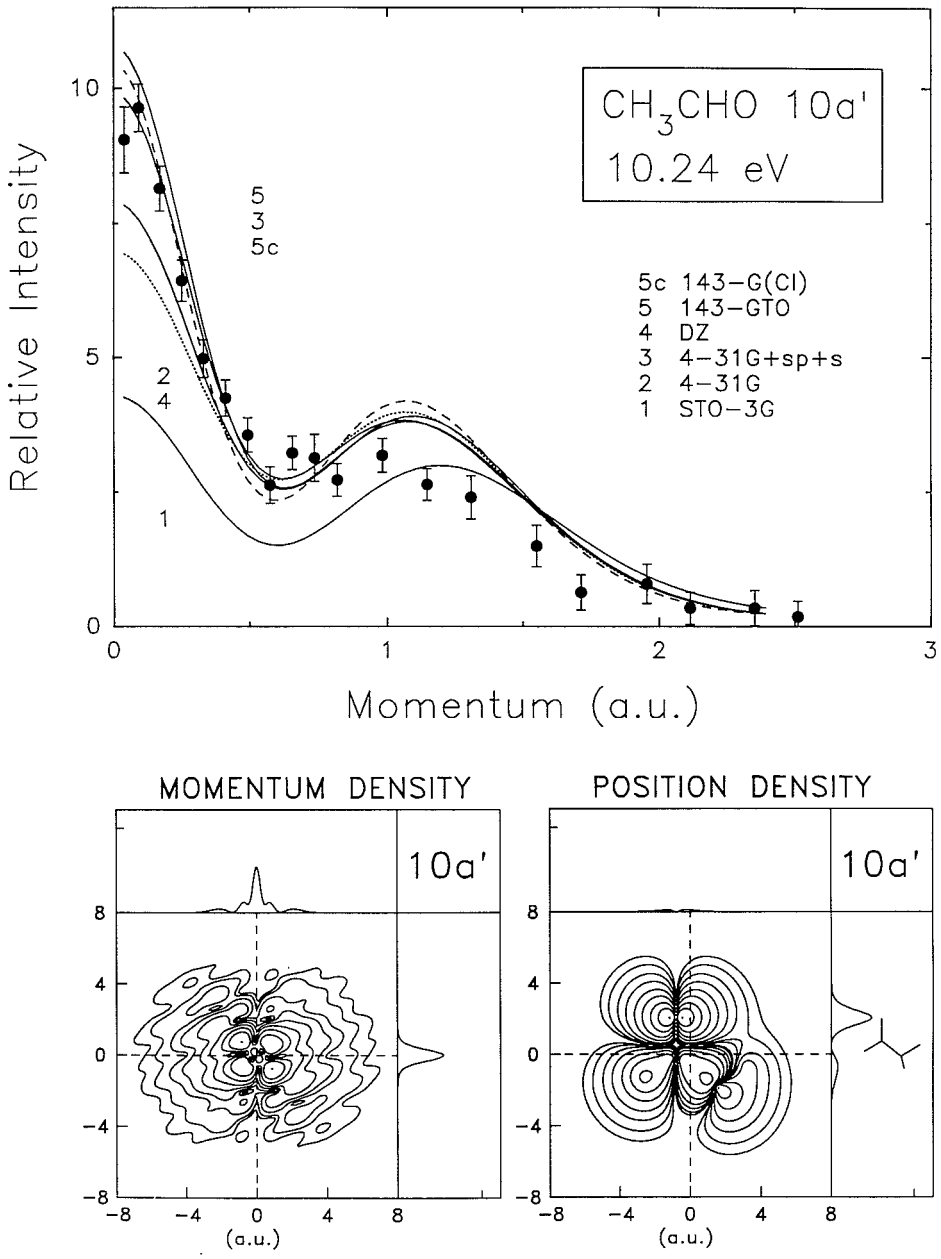

Fig. 2. Measured and calculated spherically averaged momentum profiles for the 10a′ electron of acetaldehyde (upper panel). The solid dots are the present experimental data. All calculations have been spherically averaged and folded with the experimental resolution using the GW-PG method [22] – see text (section 3 and table 1) for further details of the wavefunctions and normalization procedures. The lower panels show the momentum and position space density maps for an oriented CH_3CHO molecule calculated using the 143-GTO basis set (see section 3). The contours represent 0.01, 0.03, 0.1, 0.3, 1.0, 3.0, 10.0, 30.0, and 99.0% of the maximum density. The positions of the atoms on the position density plot (lower right panel) are located on the map. The side panels (right and top) show the density slices along the origin lines (dashed vertical and horizontal lines) for each density map.

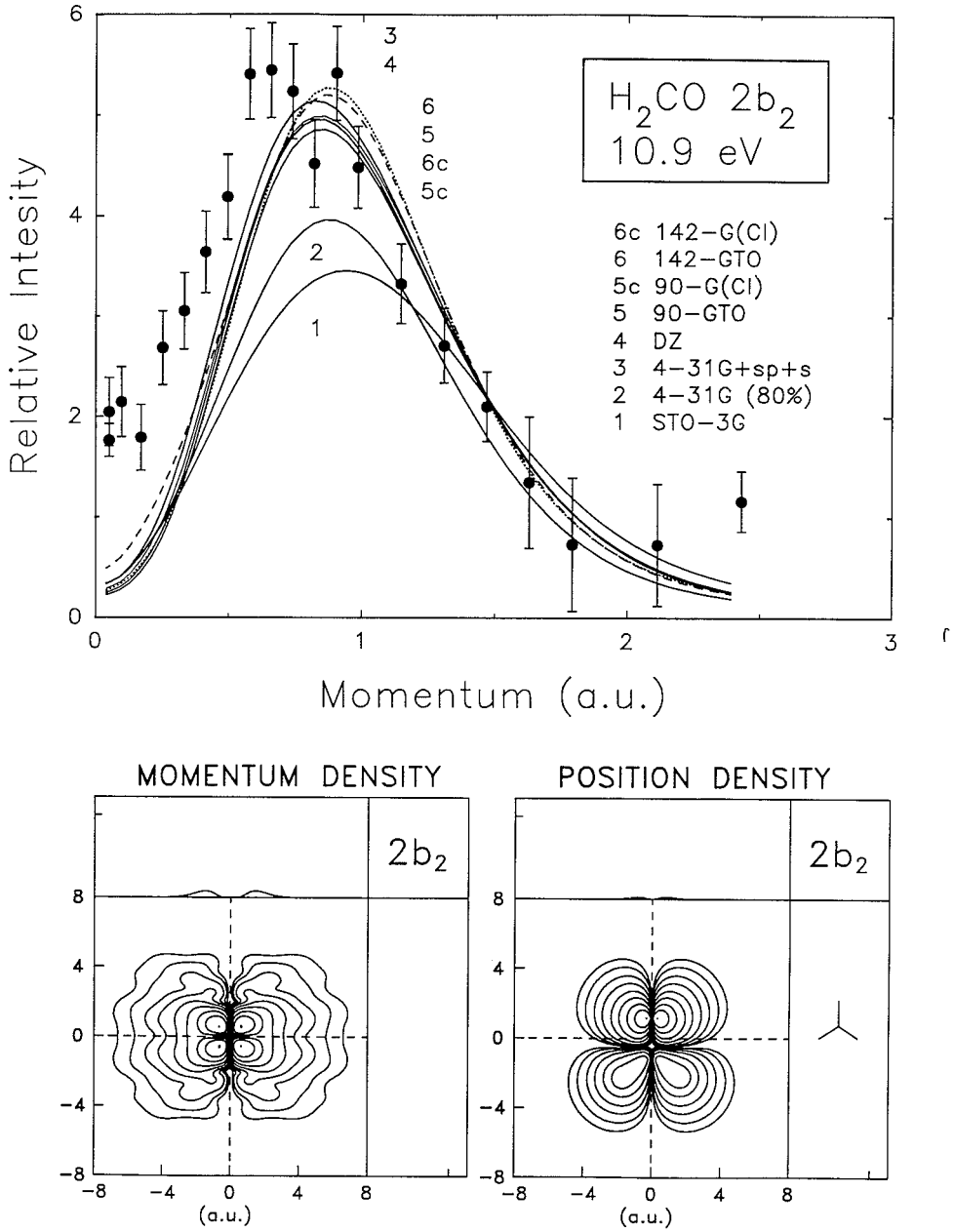

Fig. 3. Measured and calculated spherically averaged momentum profiles for the $2b_2$ electron of formaldehyde (upper panel). The solid dots are the previously reported experimental data of Bawagan et al. [20]. All calculations have been spherically averaged and folded with the experimental resolution using the GW-PG method [22] – see text (section 3 and table 1) for further details of the wavefunctions and normalization procedures. The lower panels show the momentum and position space density maps for an oriented H_2CO molecule calculated using the 90-GTO basis set (see section 3). The contours represent 0.01, 0.03, 0.1, 0.3, 1.0, 3.0, 10.0, 30.0, and 99.0% of the maximum density. The positions of the atoms on the position density plot (lower right panel) are located on the map. The side panels (right and top) show the density slices along the origin lines (dashed vertical and horizontal lines) for each density map.

distributions (TMPs) calculated from the SCF basis sets and MRSD-CI ion–neutral overlaps as described in section 3 above. Selected properties for each calculation and corresponding experimental values are shown in table 1. The SCF basis sets used range from a very modest, minimal STO-3G basis to the very much larger near-Hartree–Fock treatment. The effects of many-body correlations and electronic relaxation are also seen in figs. 1–3 from the multiple reference space singles and doubles configuration interaction calculations (MRSD-CI) of the TMPs.

It has been found in the studies of the hydrides of the row two and three main block elements and several other small molecules [4], particularly for highly polar species such as NH_3 [7], H_2O [8] and HF [9] that an accounting for the finite instrumental angular (momentum) resolution is necessary for the quantitative comparison of theoretical and experimental momentum profiles [22,46]. The recently developed, Gaussian weighted planar grid method of Duffy et al. [22] has been very successful in this regard. The EMS instrumental momentum resolution has been accounted for in all the TMPs in figs. 1–3 using this method.

The calculated momentum profiles are compared with the respective experimental momentum profiles by a visual "best fit" of the MRSD-CI TMPs with the experimental data for each molecule. All of the calculations retain their correct intensity relative to the others for each particular molecule, which allows for quantitative assessment of the wavefunctions used to generate each momentum profile. While the scales on the plots of the XMPs in figs. 1–3 are relative, the absolute calculated scale for all the spherically averaged ion–neutral overlap amplitudes (for the CI calculations using eq. (2)) and spherically averaged squares of the SCF orbitals (eq. (3)) may be obtained by dividing the relative intensity units in each figure by 100. It should also be noted that the MRSD-CI pole strength has been scaled up to one to provide a direct comparison of shape and intensity with the SCF results, which are likewise normalized such that $\int 4\pi p^2 |\psi(p)|^2 \, dp = 1$.

From figs. 1–3 it can be seen that the best descriptions of the observed momentum profiles are achieved by the high-level MRSD-CI calculation (curves 5c), noted as 90-G(CI), 143-G(CI) and 196-G(C) for formaldehyde, acetaldehyde and acetone respectively. The SCF calculations of the momentum profiles show a trend of improving agreement with experiment as the basis set quality improves from the STO-3G (curves 1) which fit the observed XMPs very poorly, to the intermediate quality results (4-31G+sp+s and DZ) and above, the near-Hartree–Fock results (curves 5, noted as 143-GTO and 196-GTO as for the MRSD-CI above), which are in good agreement with the experimental data at low momentum for acetone (fig. 1) and acetaldehyde (fig. 2). Although the statistics are poorer for acetone, nevertheless the measurements suggest that the second maximum is ≈ 0.2 au lower in momentum than predicted by the calculations for both molecules. This behaviour is quantified as the value of p_{MAX} [#1] of the momentum profile for formaldehyde, of the p_{MAX} of the second, higher momentum, "lobe" of the acetaldehyde profiles, and of the p_{MAX} values of the low- and high-momentum "lobes" in the TMPs of acetone. The calculated and estimated experimental values are shown in table 1. Note that the higher-momentum features in the acetone (at ≈ 1–1.3 au) and acetaldehyde (at ≈ 1 au) spectra (figs. 1 and 2) are not true radial lobes of the electron density since the EMS cross section does not go completely to zero between them. However, as discussed in the following section, the electronic distributions have structures that are very similar to radial nodes which are reflected in the spherical averaged density as local minima and maxima. These features will be referred to as "nodes" and "lobes" respectively, for convenience.

The minimal basis set STO-3G results are in very poor agreement with both the observed EMS data (curves 1 in figs. 1–3) and electronic properties (see table 1). For acetone and acetaldehyde the higher momentum "lobes" are of greater intensity than the lower momentum ones in clear disagreement with the experimental data. From table 1 it can be seen that as well as a poor total energy (compared with the other calculations) the calculated polarity of the C=O bond, as represented by the dipole moment, is clearly less than the observed value. These problems underline the deficiencies of a minimal basis set model.

With only a slightly larger basis set, the 4-31G

[#1] The quantity p_{MAX} refers to the momentum value at which the intensity of either an experimental or theoretical momentum profile is a maximum.

(curves 2) description provides a much better description for all three molecules than the STO-3G model. In each case the calculated momentum profiles, while shifted to higher momentum, are in qualitative agreement for shape with the XMPs. For formaldehyde [20], while not in very good agreement with the experimental data points, the 4-31G basis is almost as good as the larger, intermediate size (4-31G+sp+s and DZ, see below) basis sets. For the two larger molecules, the behaviour of the calculated momentum profiles is similar, with the 4-31G having very similar p_{MAX} values to the larger, higher-quality calculations although there is considerable intensity at higher momentum for the 4-31G TMPs than for the calculations with better total energies, particularly for acetone (fig. 1). The improvement of the 4-31G basis over the minimal description is also seen in the total energies and dipole moments in table 1. While there are obvious improvements in the respective total energies for all three molecules, the dipole moments of the 4-31G calculations are much larger than the experimental values in each case, indicating an *overestimation* of the polarity of the C=O bond. This behaviour is typical of this basis set for highly polarized bonds [7–9].

Of special interest is the behaviour of the basis sets of intermediate size, the 4-31G+sp+s basis (curves 3) and the double zeta calculation of Snyder and Basch [36] (DZ, curves 4). The extended 4-31G+sp+s basis [33,34] calculations agree particularly well with the respective XMPs, approaching the near-HF limit results, considering the relatively small size of the basis set ([4s, 3p] for O and C, [3s] for H). It must be noted, however, that the total energies and dipole moments given by this calculation (table 1), show only a small improvement over the 4-31G results and are poorer than the (smaller basis set) Snyder and Basch double zeta results.

The double zeta basis set of Snyder and Basch [36] was specifically designed to mimic two Slater functions per atomic orbital, a contracted one and a more diffuse one. As such it generally gives better agreement with the XMPs than the 4-31G TMPs (which use a more limited core orbital description) and a poorer description than the more diffuse 4-31G+sp+s TMPs. However, due to the greater number of large exponent, "core" basis functions that give a better description of the electron density near the nuclei which contributes significantly to the total energy, this basis set results in a much improved total energy and dipole moment than the extended 4-31G+sp+s basis set.

These results emphasize the care that must be taken when choosing intermediate size basis sets not very near to the Hartree–Fock minimum energy limit, particularly for the diffuse (and polarization) functions which can be tuned for specific properties. Casida and Chong [33,34] chose to add very diffuse functions (i.e. with small exponents) to the 4-31G basis which increase the electron density at long range relative to the density near the nuclei. This has the effect of improving the calculation of those properties, such as the EMS cross section (the TMPs), which depend relatively more on the large radial part of the wavefunction than the short-range part [#2]. Conversely, properties which depend on the electron density nearer the nucleus, such as total energy, do not improve proportionately. The basis set of Snyder and Basch uses larger exponents for its diffuse functions and, more importantly, an additional 'core' basis function (i.e. large exponent 1s function) for each heavy nucleus. This additional flexibility in the basis set results in a better total energy.

An examination of the momentum profiles calculated using the near-Hartree–Fock SCF basis sets (90-GTO and 142-GTO for H_2CO, 143-GTO for CH_3CHO and 196-GTO for $(CH_3)_2CO$) indicates that good agreement is attained for acetaldehyde and acetone with the experimental profiles for the low-momentum regions. At higher momentum, as with all the other SCF calculations discussed above, the intensities and p_{MAX} of the second, higher-momentum "lobes" of both acetone and acetaldehyde are overestimated (see table 1). While there is some improvement in the higher-momentum parts of the profiles for both these molecules when compared with the more limited calculations, there is still a significant difference from the experimental observations in the high-momentum regions. Previous experience

[#2] This is due to the Fourier relationship of the two spaces. Since the "period" in one space of a Fourier transform is inversely related to the "frequency" in the other, affecting the long-range radial part of a wavefunction changes the short-range momentum part and vice versa. Since the major part of the EMS cross section is at low momentum, it is emphasized by increasing diffuseness in the wavefunction.

suggests this may be due to an underestimation of the long-range parts of the electron densities for these molecules [7,8]. Use of even larger, more flexible and more diffuse basis sets might further improve the agreement with the experimental momentum profiles. The momentum profile calculated from the 90-GTO basis set for formaldehyde is considerably lower than the experimental intensity at low momentum (see fig. 3). This is consistent with the result using the 142-GTO basis set (also shown in fig. 3) of the earlier study of formaldehyde by Bawagan et al. [20]. The 142-GTO basis set has a total energy even closer to the Hartree–Fock limit. While the use of even more diffuse functions might further improve the agreement, it is possible, as with other highly polar molecules such as NH_3 [7], H_2O [8] and HF [9], that electron correlation and relaxation effects are required in order to reproduce the low-momentum component of the momentum profiles.

However, the direct calculation of the ion–neutral overlap including electron correlation and relaxation by the MRSD-CI method discussed in section 3 only slightly changes the level of agreement between the measured and calculated momentum profiles for all three molecules (figs. 1–3). In contrast to the situation for the momentum profiles, there is a significant improvement (table 1) in the calculated total energies and dipole moments. In this regard it should be remembered that the experimental values of the dipole moment involve vibrational averaging whereas the calculations are at the equilibrium geometry. Although with the inclusion of electron correlation and relaxation, there is a small change in the description of the high-momentum lobes of acetone and acetaldehyde, there is still a significant discrepancy with the XMPs. For formaldehyde, there is significant underestimation of the low-momentum cross section with little change from the SCF description of the momentum profile for either the 90-G(CI) or 142-G(CI) calculations (shown in fig. 3). The extent to which the remaining discrepancies in the case of formaldehyde are due to errors in the experiment or limitations of the calculations is, at present, unclear. Possible sources of the discrepancies in the case of the momentum profiles are the neglect of vibrational averaging (due to zero-point motion) and also the use of the plane wave impulse approximation (or PWIA, see eq. (2)). However the PWIA has been found to provide a good quantitative description in a wide variety of other EMS studies under the same kinematic conditions.

4.2. Comparison of the outermost valence momentum and position space densities of H_2CO, CH_3CHO and $(CH_3)_2CO$

A deeper appreciation for the shape of the experimental and theoretical momentum profiles may be gained by consideration of the momentum and position space electron density distribution contour maps (in the bottom panels of figs. 1–3). These calculations are based on the near-Hartree–Fock SCF results for each molecule (90-GTO for formaldehyde, 143-GTO for acetaldehyde and 196-GTO for acetone) which provide the best currently available common SCF description for all three molecules. These maps are slices of the electron density ($|\psi|^2$) in position and momentum space through the plane of the carbon and oxygen backbones of each molecule, oriented such that the C=O bonds are parallel to the vertical axes. The side panels show slices of the respective charge densities along the vertical (right panel) and horizontal (top panel) axes. For the position space maps the origin is the molecular centre of mass.

While simple valence bond descriptions predict that the outermost valence orbitals of these three molecules, H_2CO, CH_3CHO and $(CH_3)_2CO$ are nonbonding oxygen lone pairs, it is clear from the position density images (lower right panels in figs. 1–3) that these orbitals are not simply pure oxygen p structures. For all three orbitals there is considerable density located on the hydrogens and methyl groups bonded to the C=O group. The bonding character of these HOMOs is revealed by the wrinkled "cabbage section" appearance of the momentum charge density maps. This phenomenon is a reflection of the interference effects caused by multiple atomic centres participating in bonding (or anti-bonding) in the momentum space representations of the molecular orbitals. These effects are usually called bond oscillations [21,47]. In general, a highly wrinkled appearance indicates strong bonding behaviour in an orbital.

These observations indicate that the oxygen lone-pair HOMOs (H_2CO $2b_2$, CH_3CHO $10a'$, $(CH_3)_2CO$ $5b_2$) are slightly delocalized over the hydrogens for

formaldehyde and acetaldehyde and strongly diffused by the methyl groups of CH_3CHO and $(CH_3)_2CO$. Clearly, as methyl groups are substituted for hydrogens these HOMO orbitals are increasingly delocalized. A similar delocalization effect has been noticed in the previous work on the alkyl substituted amines [11–15] and on H_2O [8], CH_3OH and $(CH_3)_2O$ [17,18]. The implications of these results to an understanding of bonding in these aldehydes and ketones is discussed below.

The structures in the density maps for the oriented molecules are reflected in the spherically averaged momentum distributions. The formaldehyde $2b_2$ position map (fig. 3) clearly has C_{2v} symmetry with a nodal plane down the vertical axis, which is also preserved in the momentum space picture. When the momentum density is spherical averaged, this node, with intensity of zero at $p=0.0$ au, is reflected as a node at zero momentum in the $2b_2$ spherically averaged momentum distribution (fig. 3, upper panel). It should be noted that the non-zero intensity at zero momentum in the calculated momentum profiles in figs. 1 and 3 is due to the fact that they have been folded with the instrumental (angular) resolution function in order to compare with experiment (see section 3). Note that any intensity at $p=0$ in a spherically averaged momentum distribution (that does not include any instrumental resolution folding) must be due entirely to the s orbital components of the molecular orbital [12,15]. The Fourier relationship between the position and momentum spaces is

$$\psi(p)|_{p=0} = \frac{1}{2\pi}\int \psi(r)\, dr. \qquad (4)$$

This implies that only those atomic component orbitals which do not have equal intensity lobes of opposite sign (and thus integrate to 0) will contribute [48], such as s orbitals. The two hydrogen s orbitals make equal and opposite phase contributions to the formaldehyde $2b_2$ orbital. This gives a density of zero at zero momentum.

Given the large discrepancy between the 90-GTO near-Hartree–Fock limit SCF calculation and the observed $2b_2$ XMP at low momentum the question of how valid this independent particle model is for this "orbital" must be asked, although as noted in the previous section, the inclusion of many-body effects does not seem to significantly change agreement with the XMP. The theoretical 90-GTO results give very similar results to the 142-GTO calculations of the previous EMS study of formaldehyde by Bawagan et al. [20] for the calculated momentum profiles. A large MRSD-CI calculation using this 142-GTO basis set did not give a large change from the SCF result, as is also seen for the present 90-G(CI) calculations. It was suggested by Bawagan et al. [20] that, like the strongly polar water [8] and HF [9] molecules, very large basis sets and consideration of a great deal more configurations are necessary to adequately model the presumably highly correlated electron density in the molecular and ionic states.

Acetaldehyde, with substitution of a methyl group at one of the formaldehyde hydrogen sites, has lost the C_{2v} symmetry of formaldehyde in the 10a′ HOMO and thus the nodal plane through its centre of mass. Therefore, in momentum space there is no nodal plane and considerable density at $p=0$. Equivalently, as above, this can be described as an unbalanced atomic s orbital contribution from the hydrogen bonded to the C=O group and the methyl hydrogens. This results in a large s orbital contribution and density at $p=0$. This is observed in the corresponding XMP (fig. 2), but there is also an additional "lobe" at higher momentum. It has been suggested by Tossel et al. [13] for CH_3NH_2 and by Rosi et al. for triethylamine [14] that these higher momentum "lobes" in the experimental and theoretical momentum profiles are due to the introduction of additional nodal surfaces in the space charge density maps, when compared with simpler systems. The 143-GTO SCF calculation for CH_3CHO developed in the present work, indicates a large contribution of the methyl group carbon and the methyl hydrogens. These methyl C–H σ bonds introduce an additional nodal surface (see fig. 2) which is not present in the formaldehyde $2b_2$ map (fig. 3). When transformed into momentum space and spherically averaged, the resulting calculated momentum profile reflects this additional nodal structure as a local minimum. Both the calculations and the EMS experiment reflect this as a double "lobed" momentum profile.

The $5b_2$ orbital of acetone calculated from the 196-GTO basis set, like the formaldehyde $2b_2$ map, reflects its C_{2v} symmetry in the charge density maps in both momentum and position space (fig. 1). Equal and opposite phases on the p orbital contributions of

oxygen, the aldehydic carbon and the methyl groups result in a nodal plane along the C=O bond in r-space as was the case for the formaldehyde $2b_2$ orbital discussed above. The presence of a nodal plane through the position space centre of mass origin results in a TMP with a value of zero at $p=0$ au, which is reflected in the XMP (fig. 1, top panel). As before, this can equivalently be considered to be due to cancellation of the methyl group s components which are of opposite phase. Again, as was the case for the CH_3CHO 10a′ HOMO, the $5b_2$ XMP has a second "lobe" at higher momentum. It is evident that compared with H_2CO (fig. 3), there are two additional nodal regions caused by the methyl group a C=H bonds. As described above these result in an additional minimum at higher momentum in the calculated profiles. This is also observed in the measured momentum profile, although the position of the secondary maximum appears to be at a much lower momentum than the calculated value (see table 1).

5. Conclusions

The present work indicates that good agreement is attained between experiment and theory at low momentum for acetaldehyde and acetone using the near-Hartree–Fock limit SCF and MRSD-CI calculations developed in this work and in our previous study [20]. However the situation is less satisfactory for formaldehyde. Consideration of larger, particularly more diffuse and polarizable basis sets for SCF models may further improve the agreement at larger momentum for acetaldehyde and acetone. While inclusion of correlation and relaxation effects using a multi-reference space singles and doubles configuration interaction calculation greatly improves the total energy and dipole moments for all three molecules, there is little change in the level of agreement with the observed momentum profile. The reasons as to why the measured electron momentum profile corresponding to the removal of the $2b_2$ electron of formaldehyde is still in significant disagreement with all calculations at low momentum remain unclear.

Acknowledgement

This work received financial support from the Canadian National Networks of Centres of Excellence (Centres of Excellence in Molecular and Interfacial Dynamics), the Natural Sciences and Engineering Research Council of Canada (NSERC) and the National Science Foundation (USA). One of us (BPH) gratefully acknowledges an NSERC Postgraduate Scholarship. We are indebted to Professor L. Weiler of the Department of Chemistry at The University of British Columbia for providing the sample of acetaldehyde.

References

[1] K. Fukui, Accounts Chem. Res. 4 (1971) 57.
[2] R.B. Woodward and R. Hoffmann, The conservation of orbital symmetry (Verlag Chemie, Weinheim, 1970).
[3] C.E. Brion, Intern. J. Quantum Chem. 29 (1986) 1397, and references therein.
[4] C.E. Brion, Inst. Phys. Conf. Ser. 122 (1992) 171.
[5] C.E. Brion, P. Duffy, B.P. Hollebone, Y. Zheng and E.R. Davidson, work in progress.
[6] I. McCarthy and E. Weigold, Rept. Prog. Phys. 91 (1991) 789, and references therein.
[7] A.O. Bawagan, R. Muller-Fiedler, C.E. Brion, E.R. Davidson and C. Boyle, Chem. Phys. 120 (1988) 335.
[8] A.O. Bawagan, C.E. Brion, E.R. Davidson and D. Feller, Chem. Phys. 113 (1987) 19.
[9] B.P. Hollebone, Y. Zheng, C. E. Brion, E. R. Davidson and D. Feller, Chem. Phys. 171 (1993) 303.
[10] D. Feller, C.M. Boyle and E.R. Davidson, J. Chem. Phys. 86 (1987) 3424.
[11] A.O. Bawagan and C.E. Brion, Chem. Phys. Letters 137 (1987) 573.
[12] A.O. Bawagan and C.E. Brion, Chem. Phys. 123 (1988) 51.
[13] J.A. Tossell, S.M. Lederman, J.H. Moore, M.A. Coplan and D.J. Chornay, J. Am. Chem. Soc. 106 (1984) 976.
[14] M. Rosi, R. Cambi, R. Fantoni, R. Tiribelli, M. Bottomei and A. Giardini-Guidoni, Chem. Phys. 116 (1987) 399.
[15] C.J. Maxwell, F.B.C. Machado and E.R. Davidson, J. Am. Chem. Soc. 114 (1992) 6496.
[16] A. Minchinton, C.E. Brion and E. Weigold, Chem. Phys. 62 (1981) 369.
[17] Y. Zheng, E. Weigold, C.E. Brion and W. von Niessen, J. Electron Spectry. Relat. Phenom. 53 (1990) 153.
[18] S.A.C. Clark, A.O. Bawagan and C.E. Brion, Chem. Phys. 137 (1989) 407.
[19] R.T. Morrison and R.N. Boyd, Organic chemistry, 5th Ed. (Allyn and Bacon, Newton, 1987) pp. 202–203, 839–840, 956–959;
A. Streitweiser Jr. and C.H. Heathcock, Introduction to

organic chemistry, 3rd Ed. (MacMillan, New York, 1985) p. 197.
[20] A.O. Bawagan, C.E. Brion, E.R. Davidson, C. Boyle and R.F. Frey, Chem. Phys. 128 (1988) 439.
[21] K.T. Leung and C.E. Brion, Chem. Phys. 82 (1983) 87.
[22] P. Duffy, M. E. Casida, C.E. Brion and D.P. Chong, Chem. Phys. 159 (1992) 347.
[23] K. Takagi and T. Oka, J. Phys. Soc. Japan 18 (1963) 1174.
[24] T. Iijima and M. Kimura, Bull. Chem. Soc. Japan 42 (1968) 2159.
[25] T. Iijima, Bull. Chem. Soc. Japan 45 (1972) 3526.
[26] B.J. Garrison, H.F. Schaefer III and W.A. Lester Jr., J. Chem. Phys. 61 (1971) 3039.
[27] D.B. Neumann and J.W. Moskowitz, J. Chem. Phys. 50 (1969) 2216.
[28] J.N. Shoolery and A.H. Sharbaugh, Phys. Rev. 82 (1951) 95.
[29] P.H. Turner and A.P. Cox, J. Chem. Soc. Faraday Trans. II 74(3) (1978) 533.
[30] J.D. Swalen and C.C. Costain, J. Chem. Phys. 31 (1959) 1562.
[31] W.J. Hehre, R.F. Stewart and J.A. Pople, J. Chem. Phys. 51 (1969) 2657.
[32] R. Ditchfield, W.J. Hehre and J.A. Pople, J. Chem. Phys. 54 (1971) 724.
[33] M.E. Casida and D.P. Chong, Chem. Phys. 132 (1989) 391.
[34] M.E. Casida and D.P. Chong, Chem. Phys. 133 (1989) 47.
[35] C.L. French, C.E. Brion and E.R. Davidson, Chem. Phys. 122 (1988) 247.
[36] L.C. Snyder and H. Basch, Molecular wave functions and properties: tabulated from SCF calculations on a Gaussian basis set (Wiley, New York, 1972).
[37] H. Partridge, Near-Hartree–Fock quality GTO basis sets for the first- and third-row atoms, NASA Technical Memorandum 101044 (1989).
[38] H. Partridge, Near-Hartree–Fock quality GTO basis sets for the second-row atoms, NASA Technical Memorandum 89449 (1987).
[39] T.H. Dunning Jr., J. Chem. Phys. 90 (1989) 1007.
[40] D. Feller and E.R. Davidson, J. Chem. Phys. 74 (1981) 3977.
[41] I.L. Cooper and C.N.M. Pounder, J. Chem. Phys. 77 (1982) 5045.
[42] P. Fantucci, V. Bonačić-Koutecký and J. Koutecký, J. Comput. Chem. 6 (1985) 462.
[43] K. Kimura, S. Katsumata, Y. Achiba, T. Yamazaki and S. Iwata, Handbook of HeI photoelectron spectra of fundamental organic molecules (Halsted Press, New York, 1981).
[44] G. Bieri, L. Åsbrink and W. von Niessen, J. Electron Spectry. 27 (1982) 129.
[45] W. von Niessen, L. Åsbrink and G. Bieri, J. Electron Spectry. 27 (1982) 129.
[46] A.O. Bawagan and C.E. Brion Chem. Phys. 144 (1990) 167.
[47] J.P.D. Cook and C.E. Brion. J. Electron Spectry. 15 (1979) 233.
[48] V.G. Levin, V.G. Neudatchin, A.V. Pavlitchenkov and Yu.F. Smirnov, J. Chem. Phys. 63 (1975) 1541.